Electronic Supplementary Information for

Rational Design of a Multifunction Molecular Dye for Dual-modal NIR-II/Photoacoustic Imaging and Photothermal Therapy

Ruiping Zhang[a,b†], Yuling Xu[a†], Yi Zhang[a†], Hyeong Seok Kim[d†], Amit Sharma[d], Jing Gao[c], Guangfu Yang[a], Jong Seung Kim*[d], Yao Sun*[a]

[a] *Key Laboratory of Pesticides and Chemical Biology, Ministry of Education, International Joint Research Center for Intelligent Biosensor Technology and Health, Center of Chemical Biology, College of Chemistry, Central China Normal University, Wuhan 430079, China*

[b] *Affiliated Da Yi Hospital of Shanxi Medical University, Taiyuan 020001, China*

[c] *Jiangsu Key Laboratory of Medical Optics, Suzhou Institute of Biomedical Engineering and Technology, Chinese Academy of Sciences, Suzhou 215163, China*

[d] *Department of Chemistry, Korea University, Seoul 02841, Korea*

† These authors contributed equally to this work.

Table of Contents

General methods

All chemicals were purchased from commercial sources (such as Aldrich). The ^{1}H and ^{13}C NMR spectra were acquired on a Bruker 400 MHz magnetic resonance spectrometer. Data for ^{1}H NMR spectra are reported as follows: chemical shifts are reported as δ in units of parts per million (ppm) relative to chloroform-d (δ 7.26, s); multiplicities are reported as follows: s (singlet), d (doublet), t (triplet), q (quartet), dd (doublet of doublets), m (multiplet), or br (broadened); coupling constants are reported as a J value in Hertz (Hz); the number of protons (n) for a given resonance is indicated nH, and based on the spectral integration values. MALDI-MS spectrometric analyses were performed on an Applied Biosystems 4700 MALDI TOF mass spectrometer. UV-Vis absorbance of the probe was recorded on a Pekin Elmer Lambda 25 UV-Vis spectrophotometer. The NIR-II system was purchased from Suzhou NIR-Optics Technologies Co., Ltd. NIR-II fluorescence spectrum was recorded on an Applied Nano Fluorescence spectrometer at room temperature with an excitation laser source of 785 nm. Hydrodynamic diameter was measured using a Malvern Zetasizer Nano ZS. HPLC was performed on a Dionex HPLC System (Dionex Corporation) and a reversed-phase C18 column was used for analysis (Phenomenax, 5 μm, 4.6 mm × 250 mm) and semi-preparation (Agilent, 5 μm, 10 mm × 250 mm). Transmission electron microscopy (TEM) images were recorded on a Hitachi TEM system. TEM samples were prepared by dropping **SYL NPs** probe solution onto carbon-coated copper grids and dried at room temperature overnight without staining before measurement, the measurements were conducted with transmission electron microscopy operated at 200 kV.

General procedure for the synthesis of SYL NPs.

The nanoprobe **SYL NPs** containing the **SYL** was prepared *via* matrix-encapsulation method. Briefly, DSPE-mPEG5000 (9 mg) was dissolved in water. Then, the THF solution containing **SYL** (1 mg) was added. The mixture was then stirred at room temperature for 2 h. After THF was removed by nitrogen flow, the mixture was centrifuged at 12,000 rpm for 5 min using 30 kDa molecular weight cut-off and washed by water. After passing through a 0.2 μm syringe filter, the **SYL NPs** suspension was obtained and stored at 4 °C for further use.

Absorption spectrum and PL excitation spectra. UV-Vis-NIR absorbance of the **SYL NPs** was recorded on a PerkinElmer Lambda 25 UV-Vis spectrophotometer. PLE spectrum of the **SYL NPs** solutions were taken using an Applied Nano Fluorescence spectrometer.

Quantitative measurement of SYL encapsulated in SYL NPs. The amount of **SYL** encapsulated in the **SYL NPs** was measured by NIR absorbance spectrophotometer at 765 nm. The calibration curve was linear in the range of 5-45 μg/mL with a correlation coefficient of R^2=0.995. The encapsulated efficiency was defined as the ratio between the amount of **SYL** encapsulated in the DSPE-PEG and that added in the **SYL NPs** preparation process. The **SYL** encapsulation efficiency of **SYL NPs** was 81.6 ± 2.4 % (n=3).

Photostability test of SYL, SYL NPs and ICG NPs. The **SYL** in DMSO, **SYL NPs** in water, ICG NPs in water were irradiated by continuous 808 nm laser at the power density of 1 W/cm^2 for 60 min. Then the fluorescence intensities of **SYL**, **SYL NPs**, ICG NPs at different times were calculated manually by using ImageJ software.

The measurements of the photothermal conversion efficiency (η) of SYL and SYL NPs. The photothermal conversion efficiency (η) was calculated by following equations: τ_s is the system time constant of the sample. T_{max} (or T_{sur}) is the equilibrium temperature (or ambient temperature), I is the incident laser power (I = 1 W/cm^2), A_{808} is the sample absorbance at 808 nm.[1]

$$\eta = \frac{hs(T_{max} - T_{sur}) - Q_0}{I\left(1 - 10^{-A_{808}}\right)} \quad (1)$$

$$hs = \frac{\sum_i m_i C_{p,i}}{\tau_s} \quad (2)$$

$$\tau_s = \frac{t}{-ln\vartheta} = \frac{t}{-\ln\left(\frac{T - T_{sur}}{T_{max} - T_{sur}}\right)} \quad (3)$$

Cell line and animal model. The 4T1 cells were cultured in Dulbecco's modified Eagle's medium (DMEM) supplemented with 10% (v/v) fetal bovine serum and 1% (v/v) penicillin at 37°C and 5%

CO_2. The 4T1 tumor models were established by subcutaneous injection of 4T1 cells (1×10^6 in 100 μL of PBS) at the right-hand sides of female athymic nude mice (Suzhou Belda Bio-Pharmaceutical Co.). The mice were subjected to imaging studies when the tumor volume reached 100-150 mm^3 (about 3 weeks after inoculation). The animals have been accredited by Association for Assessment and Accreditation of Laboratory Animal Care International (AAALAC International), and all subsequent procedures were approved by and performed in accordance with the Guidelines for the Care and Use of Laboratory Animals of the Chinese Animal Welfare Committee.

In vitro Photothermal Therapy of 4TI cells with SYL NPs. To evaluate the photothermal ablation efficiency of 4T1 cells with **SYL NPs**, a standard CCK8 assay was used to measure the cell viability after laser irradiation. The 4T1 cells were seeded in a 96-well plate at a density of 5000 cells per well for 12 h in a standard cell culture atmosphere. After incubation with various treatments completed, cells treated with **SYL NPs** were irradiated with an 808 nm NIR laser (1.0 W cm^{-2}) for 0 or 5 min. Thereafter, cell viability of 4T1 was measured using a standard CCK8 assay.

Lymphatic System and Blood Vascular NIR-II Fluorescence Imaging. For lymphatic system imaging, **SYL NPs** and ICG NPs PBS solution (50 μL, 50 ug) was injected into the hindfoot pad of C57BL/6 mice (n = 3) intradermally. After injection, the lymphatic system was visualized by the NIR-II imaging apparatus. For blood vessel imaging, animals were mounted on the imaging stage in the lateral position beneath the laser. NIR-II fluorescence images were collected using a NIR-II imaging system which was purchased from Suzhou NIR-Optics Technologies CO., Ltd. The excitation light was provided by an 808-nm diode laser. The laser power density was 82 mW/cm^2 during imaging.

In vivo NIR-II Fluorescence/PA dual-modal imaging. The 4T1 tumor-bearing nude mice (n=3) were intravenously injected with **SYL NPs** (100 μL, 100 μg). NIR-II fluorescence (82 mW/cm^2, 1000 LP, 100 ms) and PA images were captured at several time points (0, 2, 8, 12, 24 h) post-injection. NIR-II fluorescence imaging collected using a NIR-II imaging system which was from Suzhou NIR-Optics Technologies CO., Ltd. PA imaging was carried out in a real-time multispectral

optacoustic tomographic (MSOT) imaging system at 765 nm.

Biodistribution analysis. Ex vivo fluorescence imaging of organs and tissues were performed with a NIR-II fluorescence imaging system with an InGaAs camera under illumination of an 808 nm laser diode at a power density of 82 mW/cm^2. 24 h after injection of **SYL NPs** for NIR-II imaging, the 4T1 tumor models (n=3) were sacrificed, the liver, kidney, tumor and other organs were collected. The NIR-II fluorescent signal of each organ was then measured by the NIR-II imaging system.

In vivo Photothermal Imaging. The nude mice bearing 4T1 tumor were intravenously injected with **SYL NPs**. The IR thermal images of tumor-bearing mice were recorded by an IR camera under continuous 808 nm laser irradiation at power densities of 1 W cm^{-2} for 5 min to investigate the *in vivo* photothermal imaging capacity of **SYL NPs**.

In vivo Photothermal Therapy. For photothermal therapy, the nude mice bearing 4T1 tumor were randomly divided into four groups (n = 3): a) PBS injection group; b) **SYL NPs** injection group (100 μg SYL); c) PBS + laser; d) **SYL NPs** + laser. After 8 h post injection, tumors were irradiated by the 808 nm laser at the power density of 1.0 W/cm^2 for 5 min for c) and d) groups and the control groups a) and b) without irradiation. During the treatment, the weights of mice were monitored every two days. The tumor lengths and widths were measured by a digital caliper every two days for over two weeks.

Chemical synthesis and characterization

General procedure for the synthesis of SYL

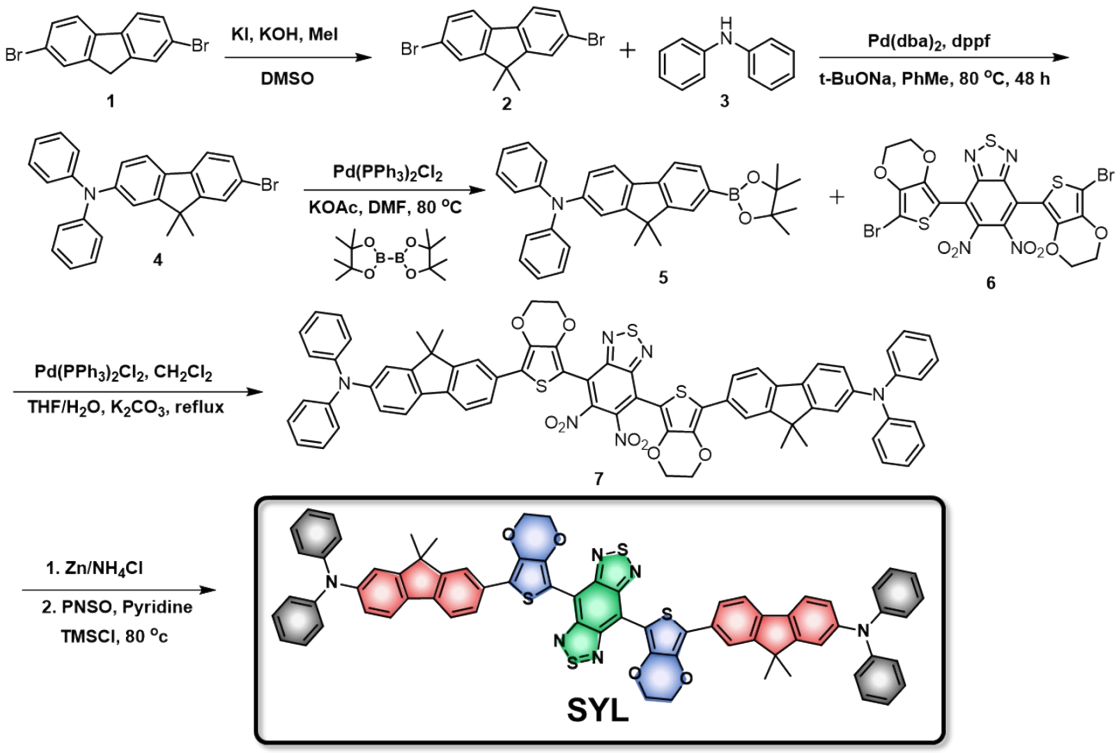

Scheme 1. Total **s**ynthetic scheme of **SYL**.

Synthesis of compound 2

1 (2.00 g, 6.17 mmol) and potassium iodide (204.84 mg, 1.23 mmol) were dissolved in anhydrous dimethyl sulfoxide (25 mL) under an argon atmosphere. Methyl iodide (2.00 mL, 13.57 mmol, 1.92 g) was added to the reaction mixture dropwise. Further, potassium hydroxide (1.73 g, 30.85 mmol) was added in 10 portions to the solution. The green reaction mixture was stirred at room temperature for 24 h and quenched with water. The mixture was acidified to pH 5 with 2 M aq. HCl solution, extracted with ethyl acetate(3×150 mL). The combined organic layers were dried with anhydrous magnesium sulfate (Mg_2SO_4), filtered and concentrated. Compound **2**(1.73g, 79.7%) obtained as a white solid was used as such for next step without furtherpurification.^{1}H NMR (400 MHz, $CDCl_3$) δ 7.58 – 7.55 (m, 4H), 7.48 (dd, J = 8.1, 1.5 Hz, 2H), 1.49 (s, 6H); ^{13}C NMR (101 MHz, $CDCl_3$) δ 155.28, 137.18, 130.35 , 127.20, 121.49, 47.34, 26.87.

Synthesis of compound 4

To an oven-dried 100 mL Schlenk tube, **2** (200mg, 0.568mmol), diphenylamine(67.35mg,0.398 mmol), bis(dibenzylideneacetone)palladium $Pd(dba)_2$, (4.9 mg, 0.0085 mmol), 1,2-bis(diphenylphosphino)ferrocene (dppf, 4.72 mg, 0.0085 mmol), sodium *t*-butoxide (54.6 mg, 0.568 mmol) and toluene (20 mL) were sequentially added. The resulting reaction mixture was stirred at 80 °C for 2 days. After cooling to room temperature, water (20 mL) and AcOEt (100 mL) were added to the reaction mixture. The organic phase was separated, and the aqueous layer was extracted with ethyl acetate (2 × 100 mL). The combined organic extracts were washed with water (20 mL) and brine (20 mL), dried over anhydrous Na_2SO_4, and concentrated under reduced pressure. The residue was purified by flash column chromatography on silica gel (eluent: *n*-hexane/AcOEt (50:1)), obtaining the product **4** (114mg, 65% yield based on diphenylamine).^{1}H NMR (400 MHz, $CDCl_3$) δ 7.60 – 7.44 (m, 4H), 7.38 – 7.24 (m, 4H), 7.22 – 7.15 (m, 5H), 7.07 (t, *J* = 7.3 Hz, 3H), 1.43 (s, 6H); ^{13}C NMR (101 MHz, $CDCl_3$) δ 147.47, 147.30, 144.92, 138.26, 137.69, 132.33, 129.76, 129.39, 125.68, 124.80, 123.85, 123.06, 115.23, 114.49, 62.46, 26.23.

Synthesis of compound 5

To a solution of **4** (836.1mg, 1.89 mmol), bis(pinacolate)diboron (863.9mg, 3.40mmol) and KOAc (445.2 g, 4.54 mmol) and in DMF (15 mL) was added bis(triphenylphosphine)palladium(II) dichloride (134.0 mg, 0.496 mmol) under an argon atmosphere. Then the reaction mixture was heated in an oil bath at 85 °C for 12 h. The reaction mixture was cooled down to room temperature, ethyl acetate (60 mL) was added and solid was removed by filtration. The solution was diluted with water (120 mL) and extracted with *n*-hexane (3×60 mL). The combined organic layers were washed with water (4×60 mL), saturated aqueous brine (150 mL) and dried over anhydrous $MgSO_4$. The solvents were concentrated to 4 mL and cooled to -20 °C to obtain compound **5** as yellow solid (665.7mg , yield 72%).^{1}H NMR (400 MHz, $CDCl_3$) δ 7.93 – 7.86 (m, 2H), 7.69 (d, *J* = 7.6 Hz, 1H), 7.64 (d, *J* = 8.2 Hz, 1H), 7.30 (dd, *J* = 14.6, 7.1 Hz, 4H), 7.20 (d, *J* = 7.7 Hz, 4H), 7.10 – 7.04 (m, 3H), 1.44 (s, 6H), 1.33 (s, 12H); ^{13}C NMR (101 MHz, $CDCl_3$) δ 155.80, 152.69, 147.95, 142.12, 134.82, 134.09, 133.75 , 129.31, 124.30, 123.09, 122.85, 121.16, 118.82, 118.27, 83.67, 46.85, 27.20 , 25.21, 24.67.

Synthesis of compound 7

To a solution of **5** (200 mg, 0.41 mmol) and **6** (123.38 mg, 0.18mmol) in THF (8.0 mL),argon gas was bubbled for 5 min. Potassium carbonate (70.8mg, 0.175 mmol) in 2.0 mL distilled water and 1,1'-Bis(diphenylphosphino) ferrocenepalladium(II)dichloride dichloromethane complex (33.62 mg, 0.041mmol) were added to the above reaction mixture under an argon atmosphere. The mixture was heated in an oil bath at 75 °C for 8 h. After cooling to room temperature, the solvent was removed in vacuum. The residue was dissolved in dichloromethane, and the resulting solution was washed with water, saturated aqueous brine. After drying over anhydrous $MgSO_4$, filtration and removal of the solvents under reduced pressure, product **7** (159 mg, 63% yield) was obtained as a dark purple solid which can be used in the next step without further purification.^{1}H NMR (400 MHz, $CDCl_3$) δ 7.79 (d, *J* = 7.4 Hz, 4H), 7.64 (d, *J* = 8.4 Hz, 2H), 7.57 (d, *J* = 8.2 Hz, 2H), 7.27 (dd, *J* = 10.2, 5.3 Hz, 8H), 7.19 (d, *J* = 1.4 Hz, 2H), 7.15 (d, *J* = 7.9 Hz, 8H), 7.03 (t, *J* = 7.0 Hz, 6H), 4.39 (d, *J* = 3.0 Hz, 4H),

4.29 (s, 4H), 1.24 (s, 12H); ^{13}C NMR (101 MHz, $CDCl_3$) δ 155.49, 154.06, 152.64, 148.86, 147.80 , 142.99 , 142.80 , 138.89 , 137.37, 133.43, 130.18, 129.27, 128.78, 126.56, 125.79, 125.08 , 124.26, 123.00 , 122.60 , 120.72 , 119.59, 118.31, 102.46, 75.08, 64.54, 46.99, 27.13, 24.87.

Synthesis of SYL

Zinc dust (502 mg, 7.68 mmol) and NH_4Cl (132.24 mg, 2.3 mmol) were added to a stirred solution of **6** (79 mg, 0.064 mmol) in dichloromethane (10 mL) and 90% methanol (9.5 mL) under an argon atmosphere. After being stirred at room temperature for 4 h, the solution was filtered through Celite pad, diluted with dichloromethane, and washed with water, saturated aqueous $NaHCO_3$, and brine. The organic phase was dried over anhydrous $MgSO_4$, filtered and concentrated under vacuum to afford a yellow solid which was utilized for the next step without further purification.

To a dark yellow solution in anhydrous pyridine (1 mL) was added *N*-thionylaniline (0.25 mL, 2.24 mmol, 307.5 mg) and chlorotrimethylsilane (0.36 mL, 4.3 mmol, 453.6 mg). The mixture was heated in an oil bath at 80°C for 20 h. The reaction mixture was allowed to cool down to room temperature, poured into ice water, extracted with dichloromethane. The combined organic layer was washed with water, saturated aqueous brine, dried over anhydrous $MgSO_4$, and concentrated in vacuo. The residue was purified by flash column chromatography on silica gel (5:1 petroleum ether: ethyl acetate) to yield the product **SYL** as a green solid (32.1 mg, two step 42 % yield).^{1}H NMR (400 MHz, $CDCl_3$) δ 7.86 (d, J = 10.0 Hz, 4H), 7.68 (d, J = 7.5 Hz, 2H), 7.60 (d, J = 7.8 Hz, 2H), 7.29 (s, 10H), 7.19 (t, J = 11.5 Hz, 10H), 7.06 (d, J = 6.1 Hz, 6H), 4.54 (s, 4H), 4.40 (s, 4H), 1.28 (s, 12H); ^{13}C NMR (101 MHz, $CDCl_3$) δ 171.60 , 152.64 , 143.20 , 142.86, 140.73, 140.22, 137.44, 129.66 , 126.14, 125.31, 122.87, 120.58 , 119.57 , 118.35 , 108.83 , 106.76, 102.81, 64.59 , 63.28, 38.83 , 33.70 , 17.17.

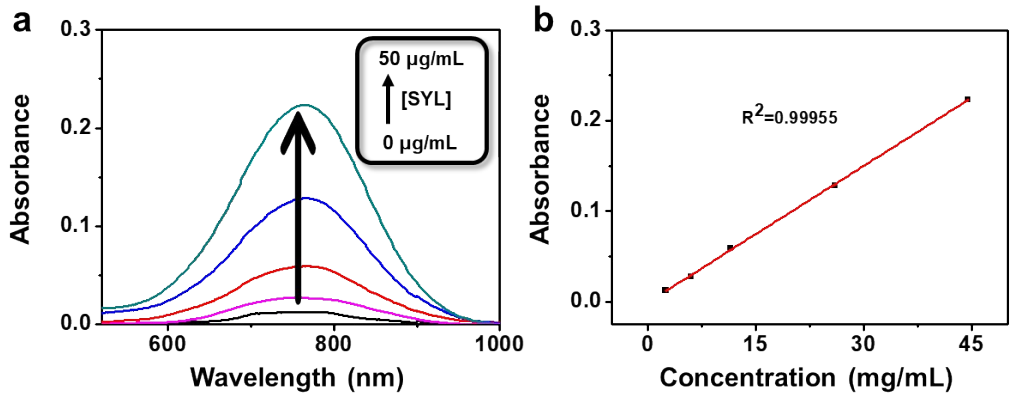

Figure S1. The calibration curve of **SYL NPs**. The amount of **SYL** encapsulated in the DSPE-mPEG5000 was measured by UV-VIS spectrophotometer at 765 nm. The calibration curve was linear in the range of 5–45 µg/ml with a correlation coefficient of $R^2 = 0.999$. The encapsulation efficiency was defined as the ratio between the amount of **SYL** encapsulated in the DSPE-mPEG5000. The organic dye **SYL** encapsulation efficiency of **SYL** NPs was 81.6 ± 2.4%.

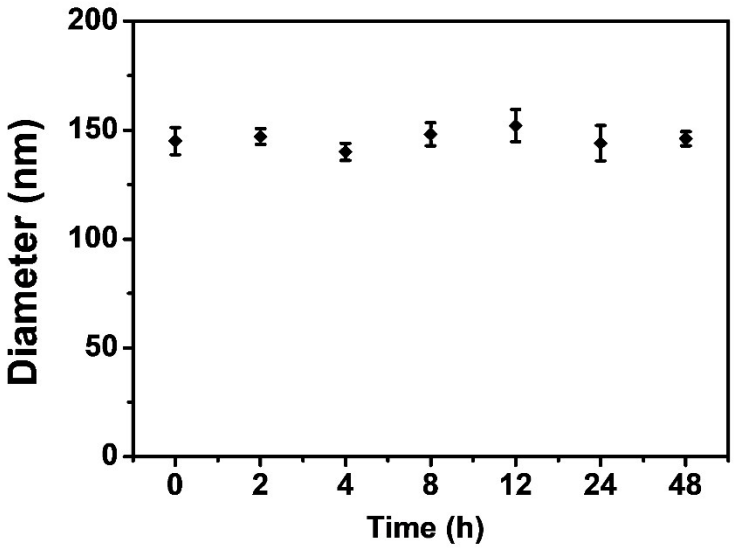

Figure S2. The *in vitro* stability of **SYL NPs** in PBS (0.5 mg/mL) containing 10% Fetal Bovine Serum (FBS) after various incubation times, the average diameters of **SYL NPs** were determined by DLS measurements.

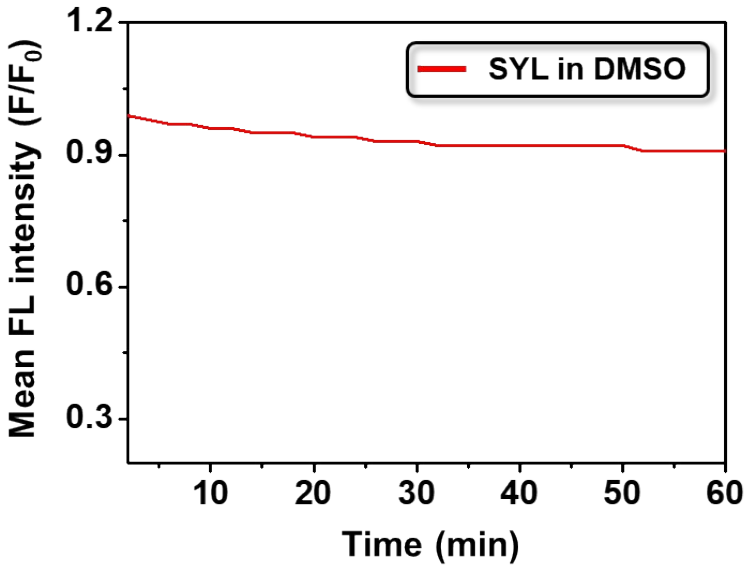

Figure S3. The photo-stability of **SYL** in DMSO under continuous 808 nm laser irradiation (10 ms, 1000 LP, 1.0 W/cm^2).

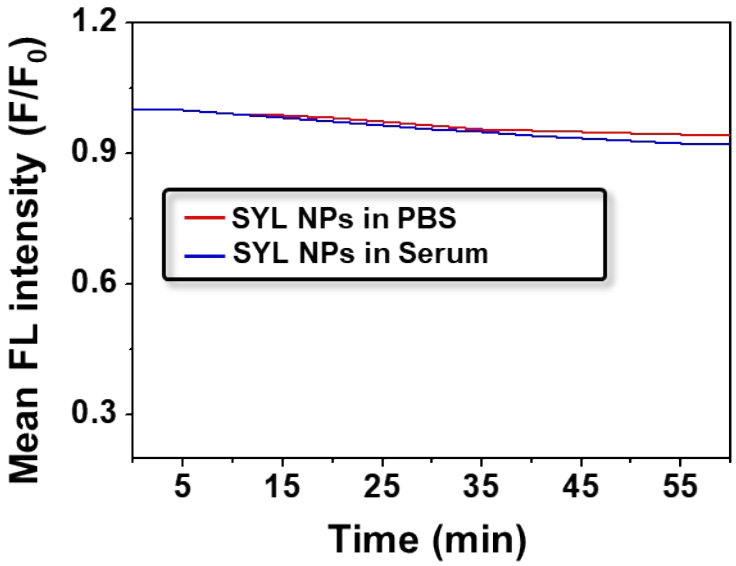

Figure S4. The photo-stability of **SYL NPs** in different mediums under continuous 808 nm laser irradiation (10 ms, 1000 LP, 1.0 W/cm^2).

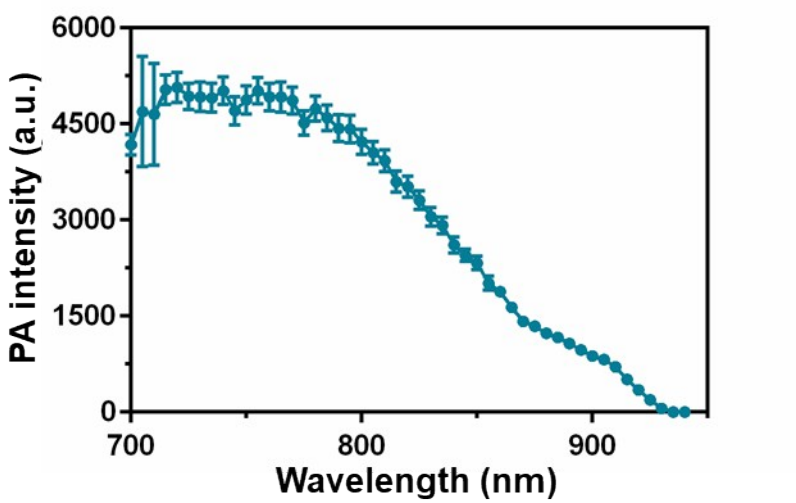

Figure S5. PA spectra of **SYL NPs** in aqueous solution (100 μg/mL).

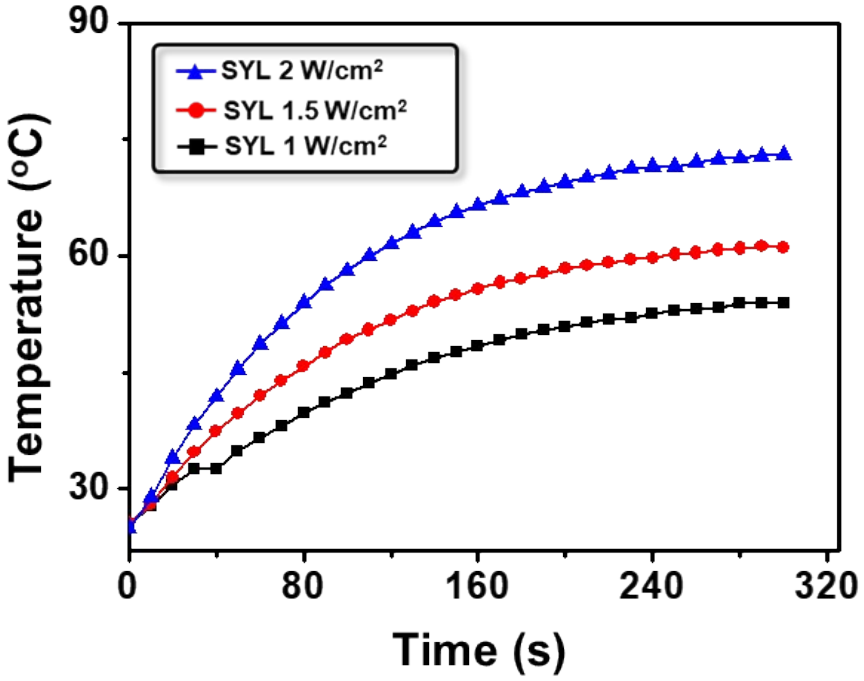

Figure S6. Photothermal conversion behavior of **SYL** NPs (12.5 μg/mL) in PBS solution at various laser power (808 nm).

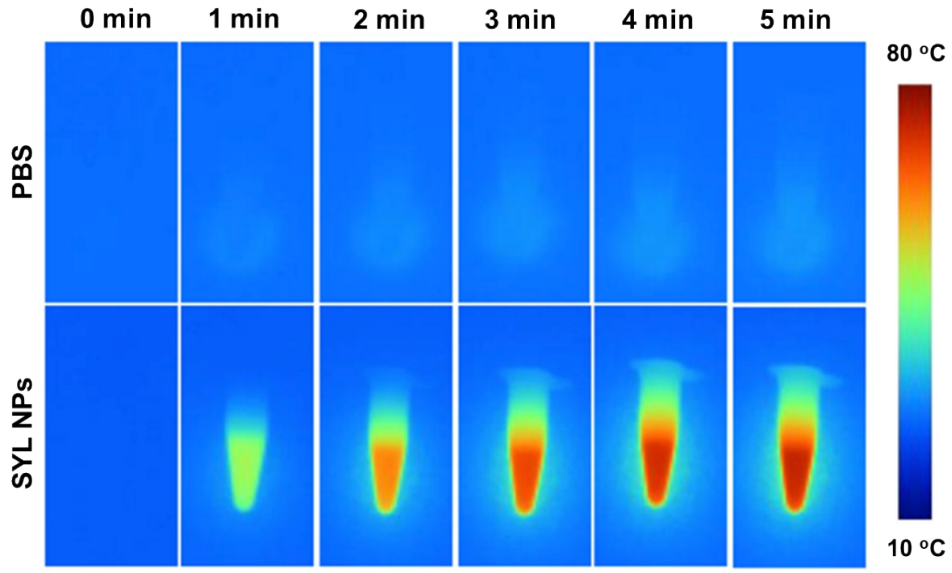

Figure S7. IR images of **SYL** NPs (50 μg/mL) in PBS solution under different irradiation time (808 nm).

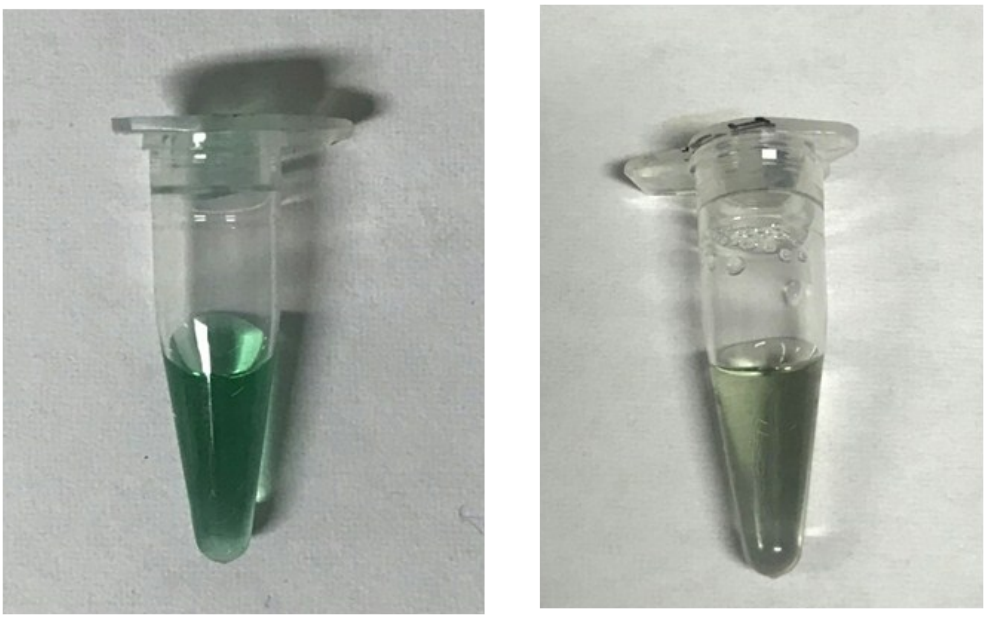

Figure S8. Photo images of ICG NPs (25 μg/mL) in PBS solution before and after photothermal heating and natural cooling for 5 cycles (1 W/cm^2).

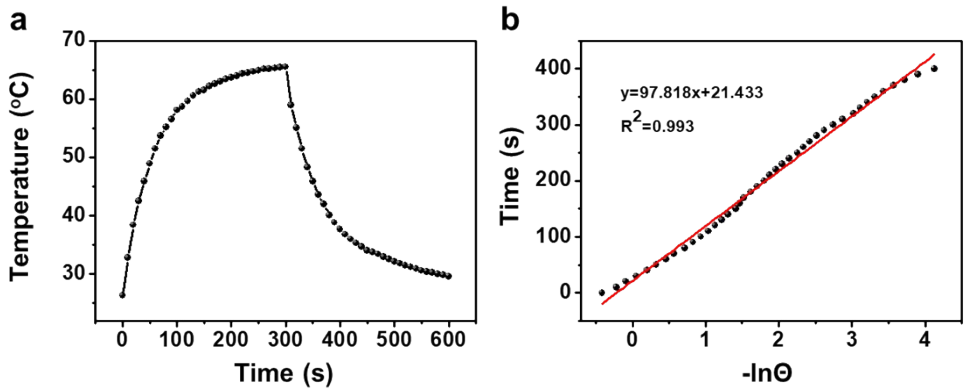

Figure S9. a) The heating and nature cooling curve of **SYL** in DMSO (30 μg/mL) under 808 nm laser irradiation; b) Linear time data versus -lnθ from the cooling period of figure S9a.

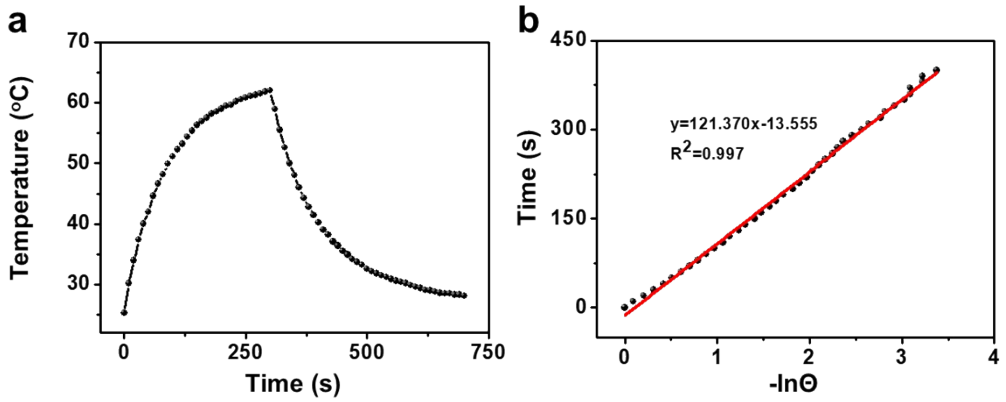

Figure S10. a) The heating and nature cooling curve of **SYL NPs** in PBS solution (30 μg/mL) under 808 nm laser irradiation; b) Linear time data versus -lnθ from the cooling period of figure S8a.

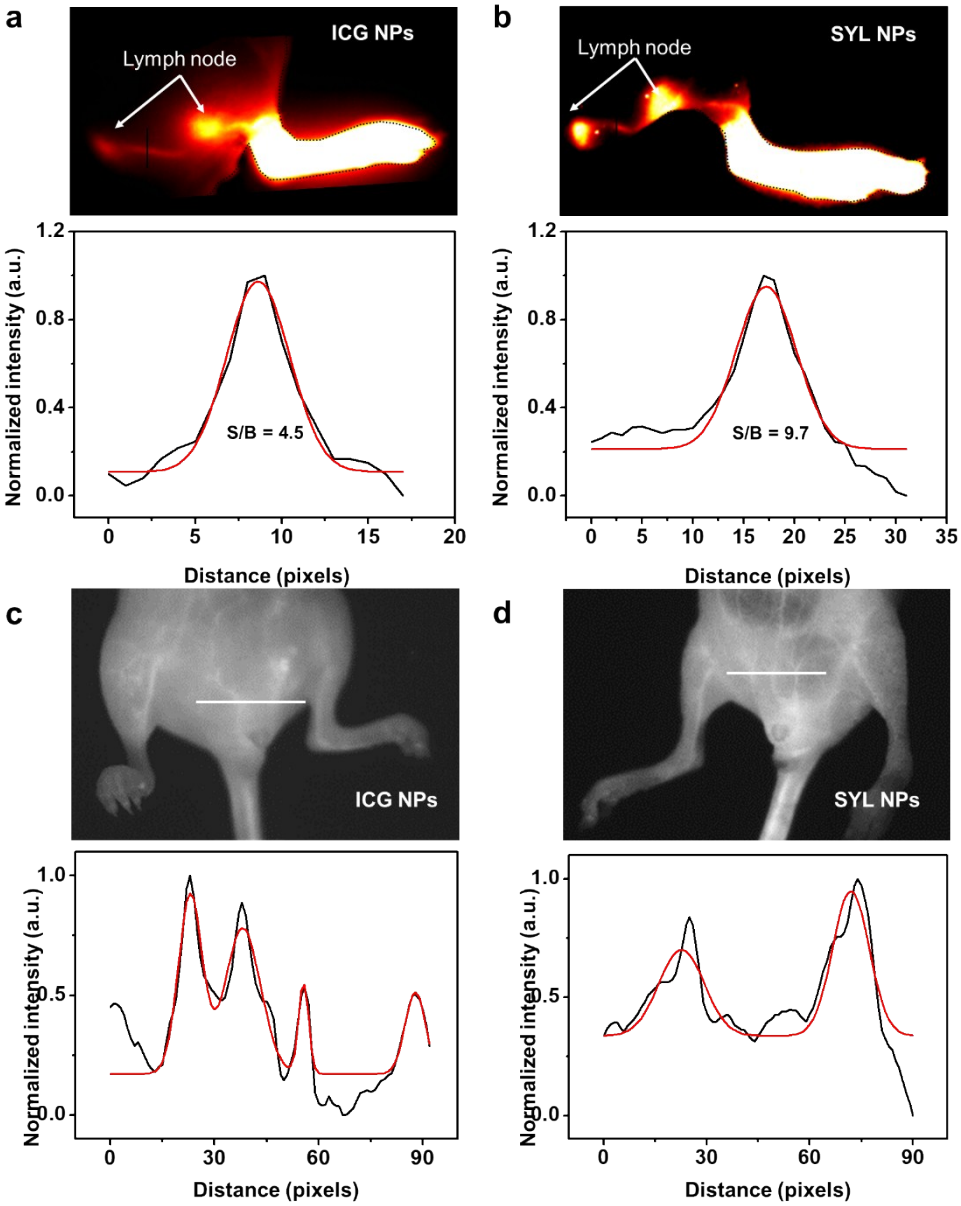

Figure S11. NIR-II lymph vessels images of ICG NPs a) and **SYL** NPs b); NIR-II vessels images of ICG NPs c) and **SYL** NPs d). (20ms, 1000 LP for **SYL** NPs, 880 LP for ICG NPs, 82mW/cm^2).

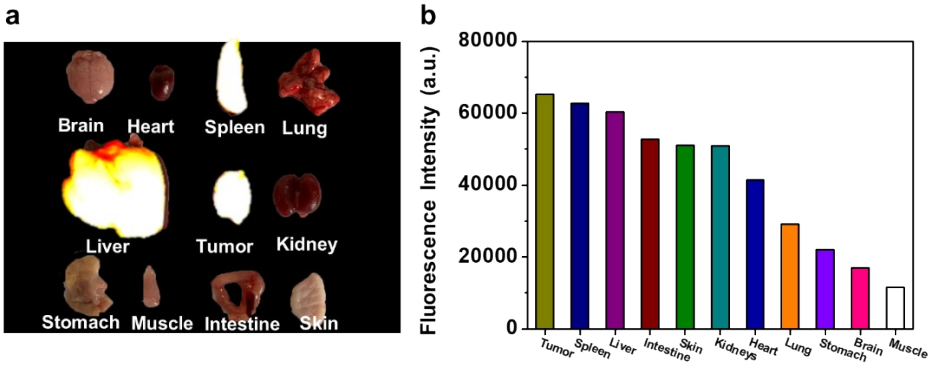

Figure S12. a) *Ex vivo* biodistribution of **SYL NPs** recorded after 24 h post injection under 808 nm laser illumination (82 mW/cm^2, 50 ms, 1000 LP); b) NIR-II signals intensity of major organs *ex vivo*.

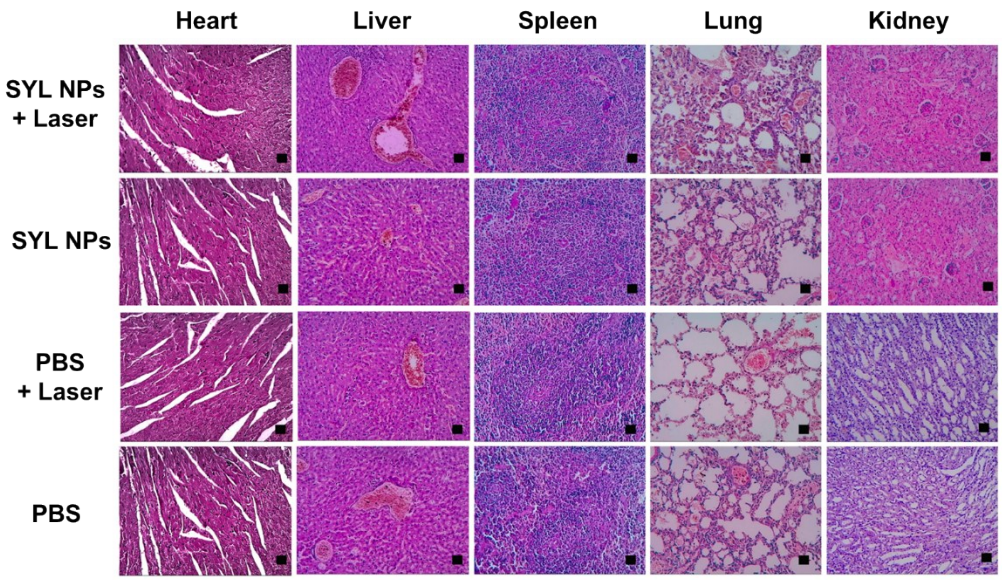

Figure S13. Histological analysis. H&E staining of major organs like hearts, livers, spleens, lungs and kidneys of mice treated with different formulations (PBS, PBS + laser, **SYL** NPs only and **SYL** NPs + laser).

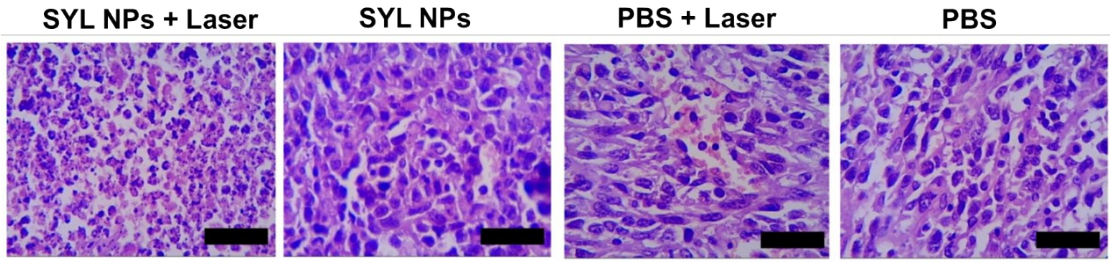

Figure S14. H&E stains of tumor from mice treated with different formulations. (800 x magnification)

NMR Spectra

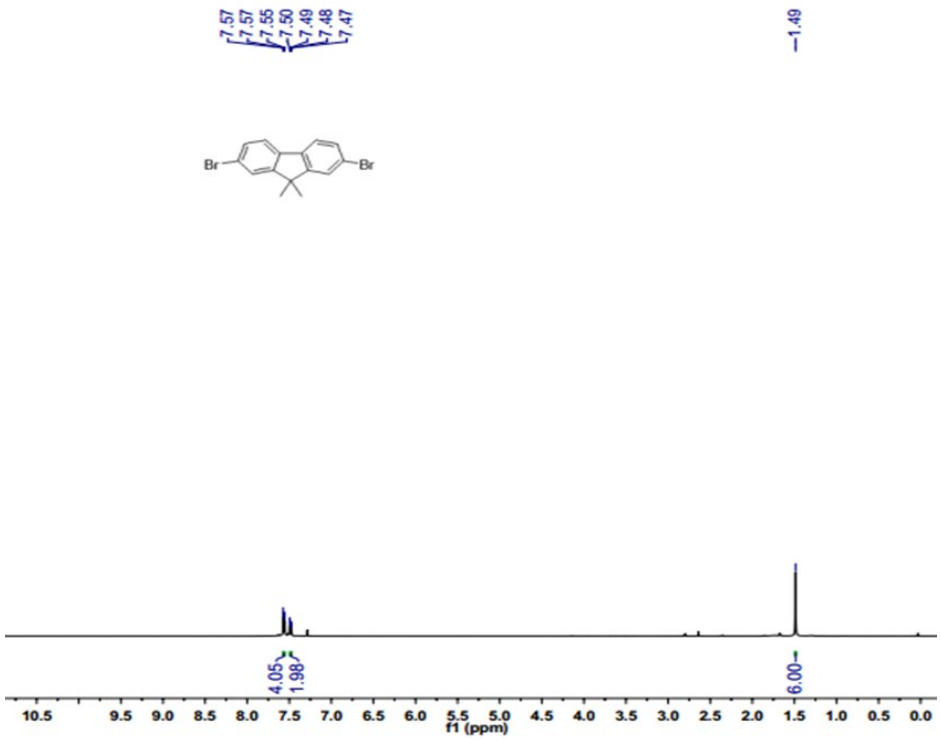

Figure S15. ^{1}H-NMR spectrum of **2**.

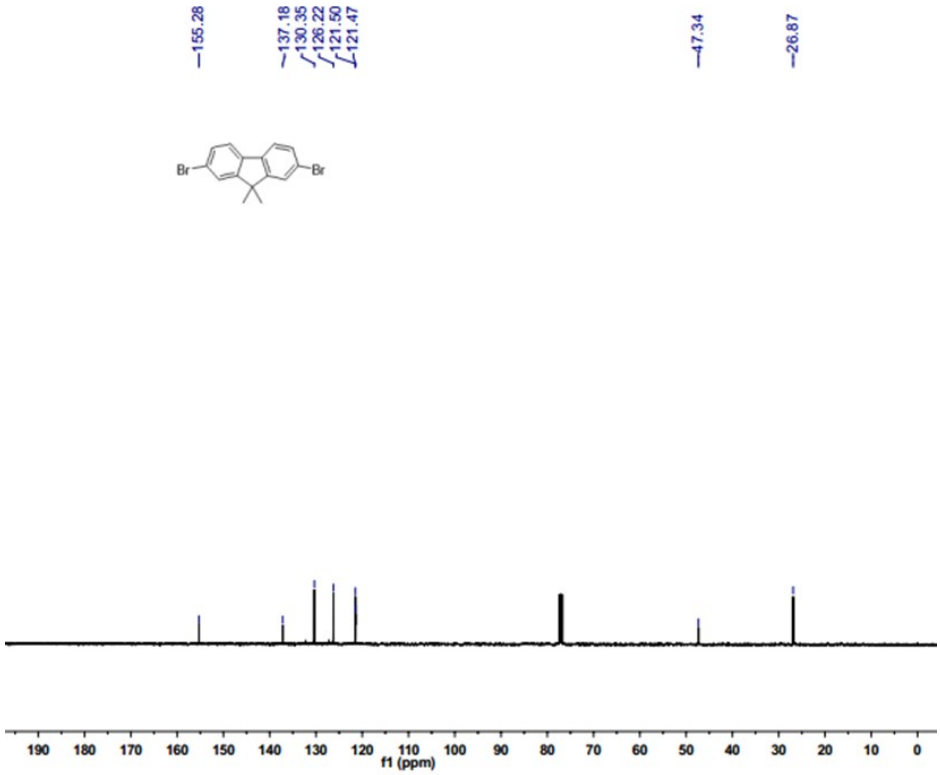

Figure S16. ^{13}C-NMR spectrum of **2**.

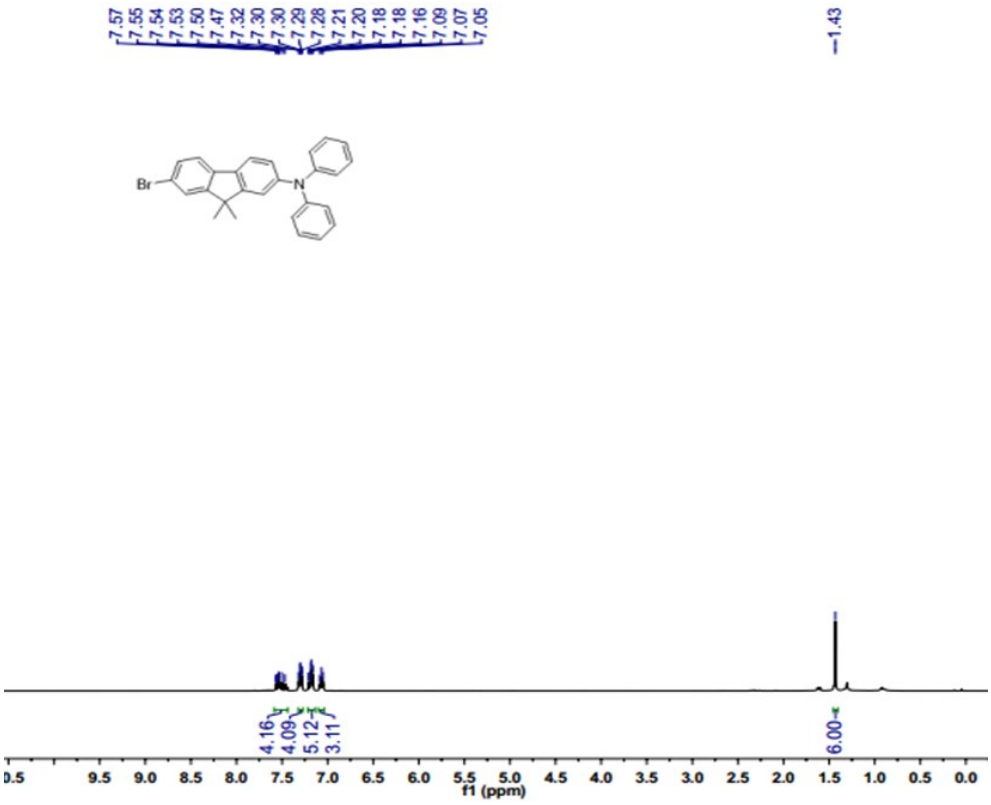

Figure S17. ^{1}H-NMR spectrum of **4**.

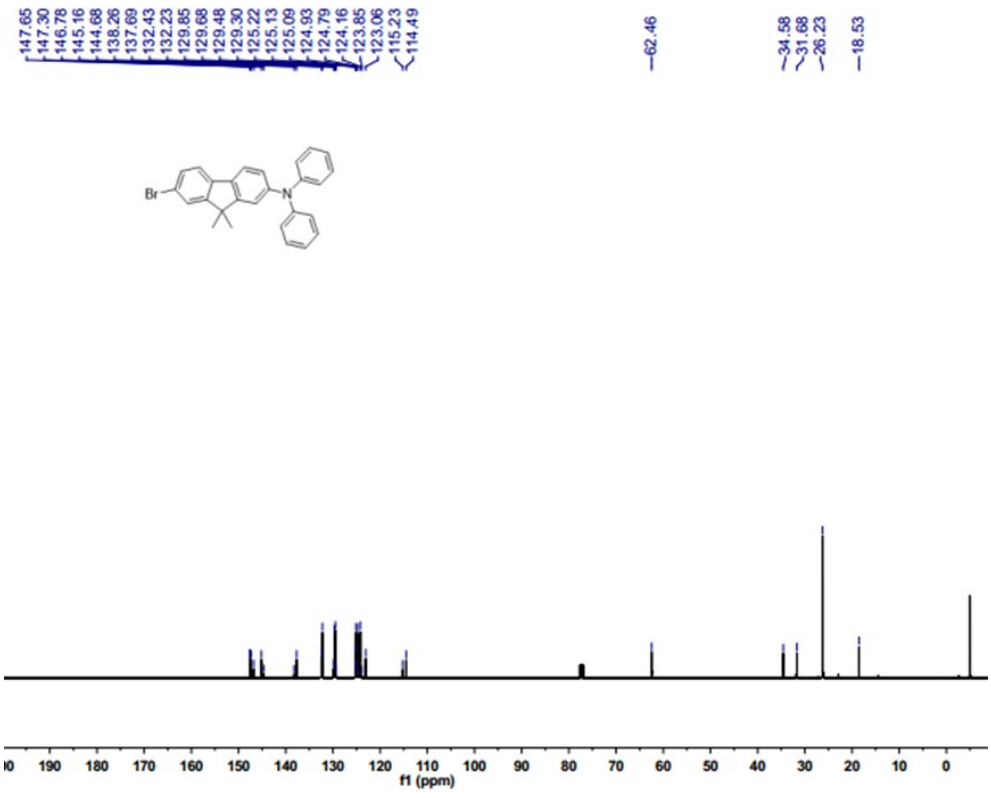

Figure S18. ^{13}C-NMR spectrum of **4**.

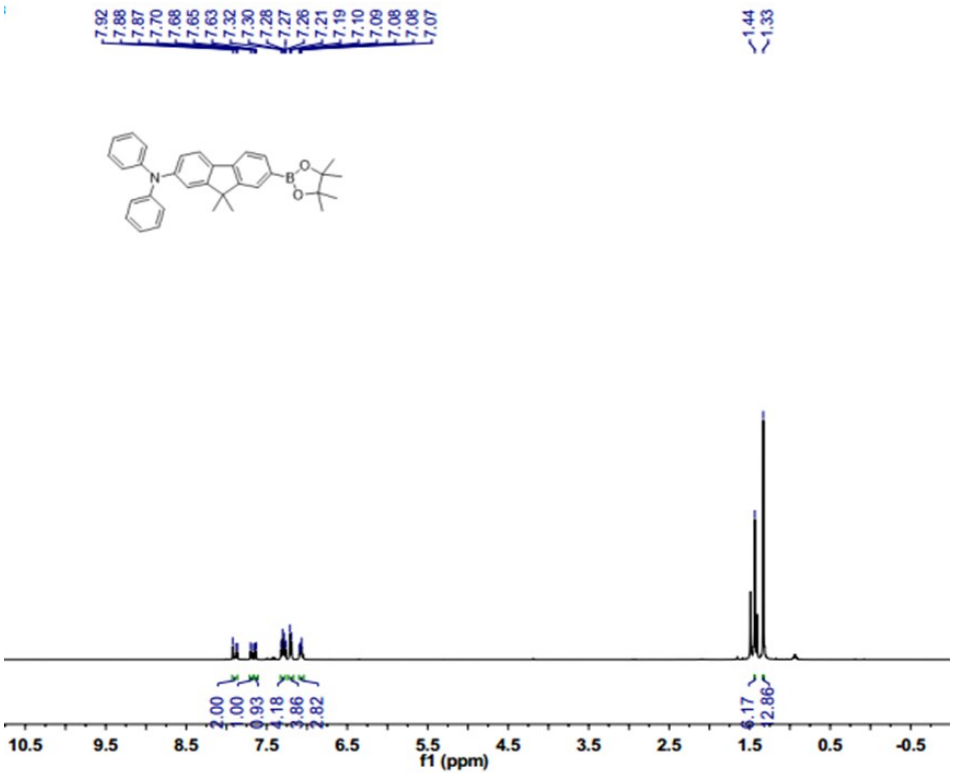

Figure S19. ^{1}H-NMR spectrum of **5**.

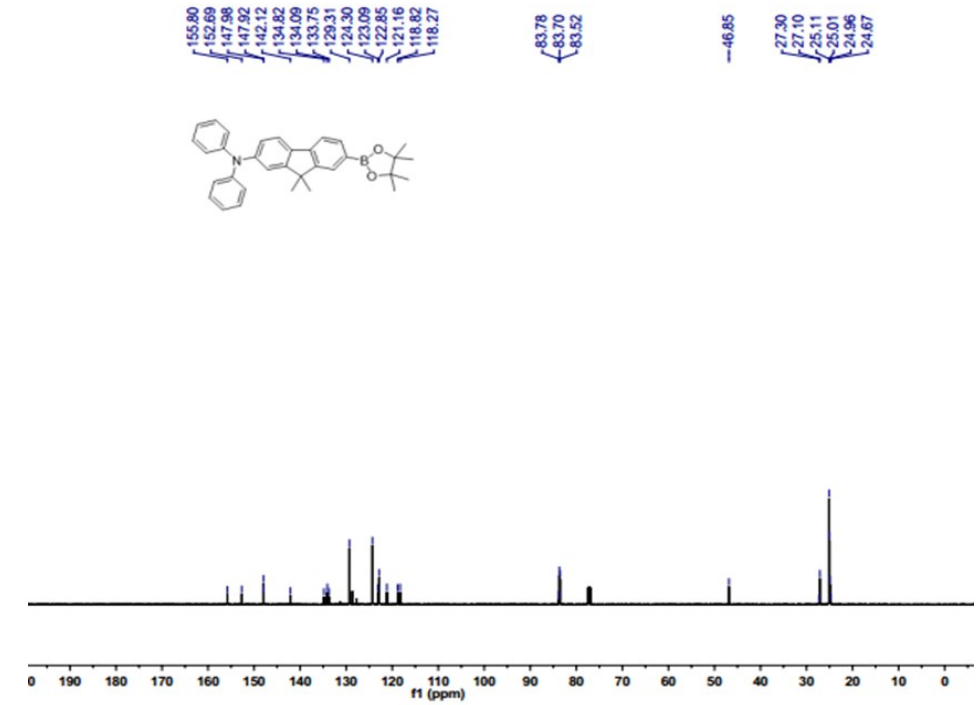

Figure S20. ^{13}C-NMR spectrum of **5**.

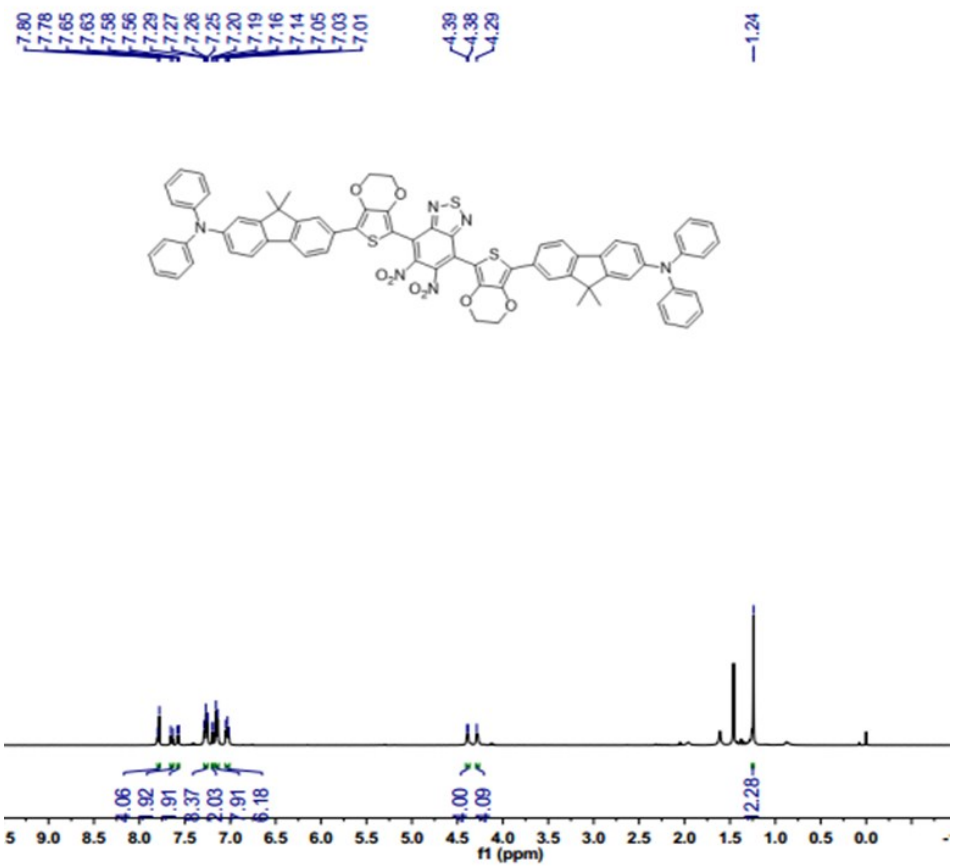

Figure S21. ^{1}H-NMR spectrum of **7**.

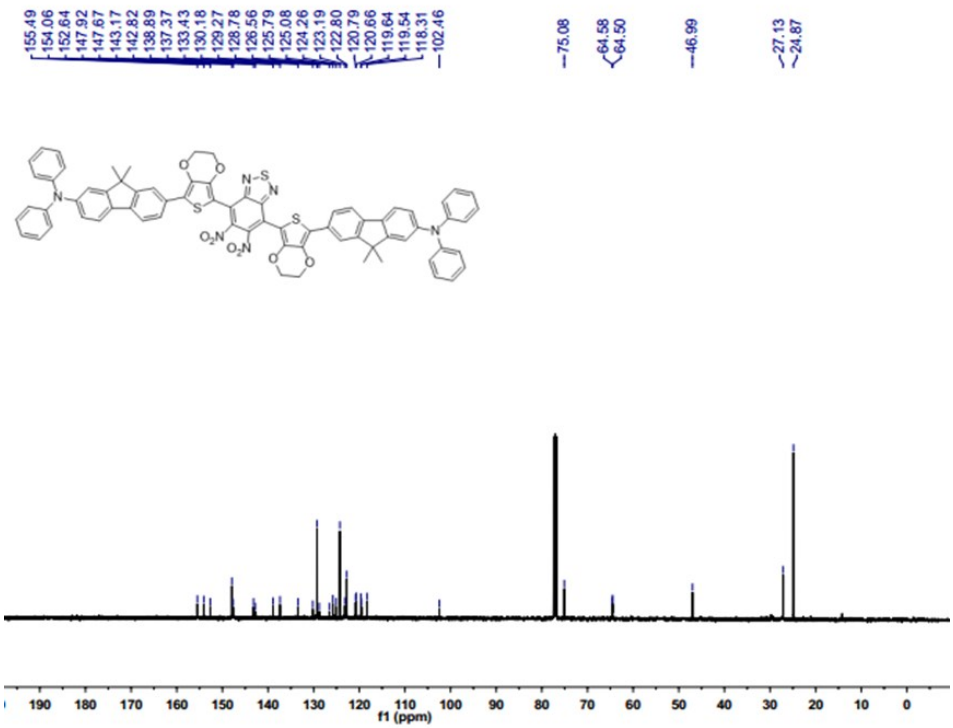

Figure S22. ^{13}C-NMR spectrum of **7**.

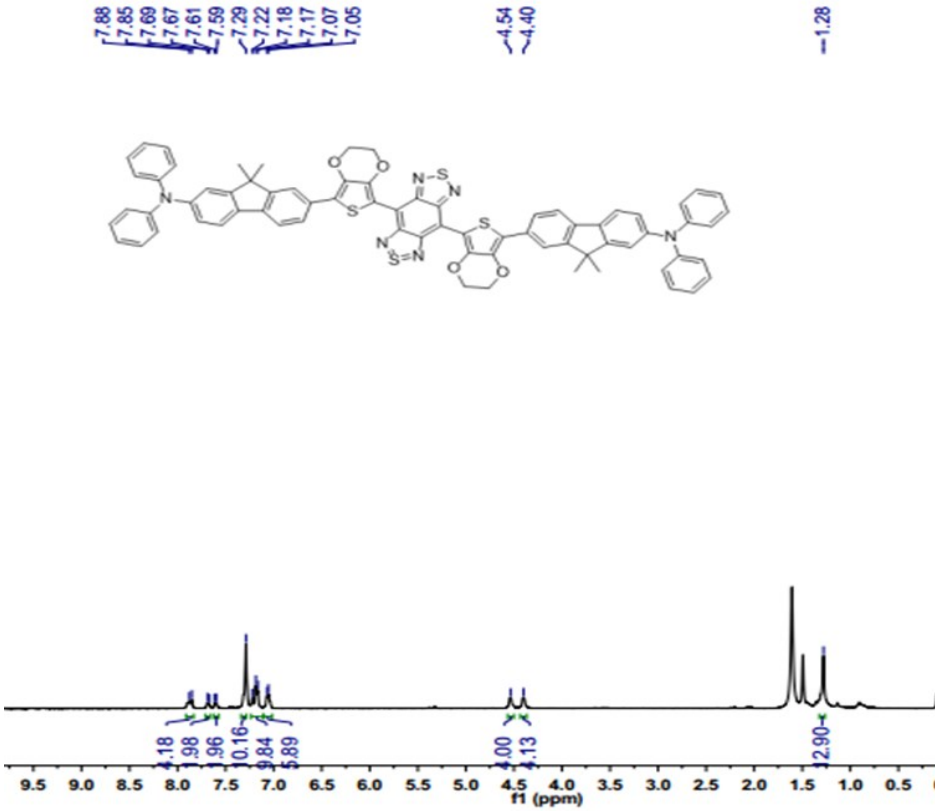

Figure S23. ^{1}H-NMR spectrum of **SYL**.

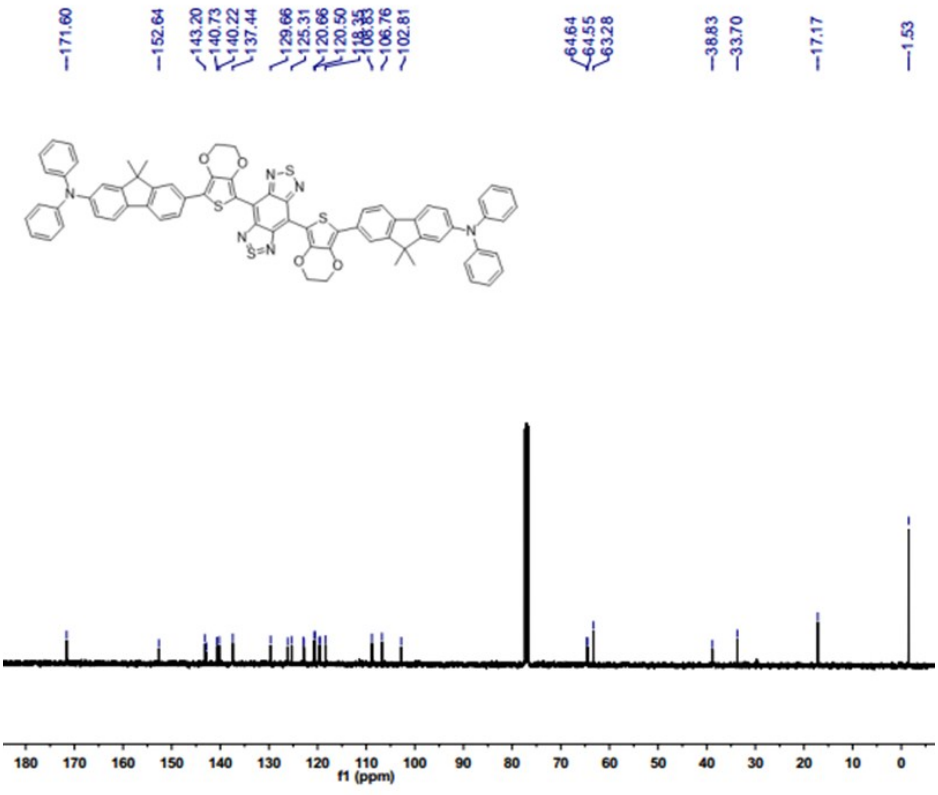

Figure S24. ^{13}C-NMR spectrum of **SYL**.

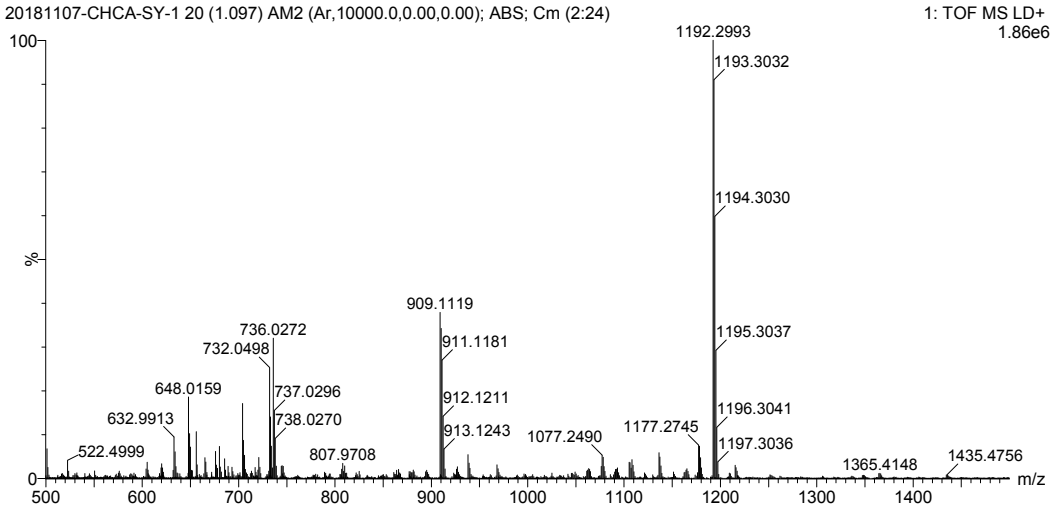

Figure S25. MALDI-TOF-MS of **SYL**

Reference

1. Q. Tian, F. Jiang, R. Zou, Q. Liu, Z. Chen, M. Zhu, S. Yang, J. Wang, J. Wang and J. Hu, *ACS Nano*, 2011, **5**, 9761-9771.